PAPER

Effect of MoO₃ buffer layer on the electronic structure of Al–BP interface

To cite this article: Baoxing Liu et al 2022 J. Phys. D: Appl. Phys. 55 364005

View the article online for updates and enhancements.

You may also like

- <u>Spin coating preparation and thermal properties of metastable Al/PVDF energetic film with graphene</u>
 Liang Guo, Yajun Wang, Pengfei He et al.
- Research on the hydrogen terminated single crystal diamond MOSFET with MOO₃ dielectric and gold gate metal Zeyang Ren, Jinfeng Zhang, Jincheng Zhang et al.
- Role of Potassium Permanganate-Based Solutions in Controlling the Galvanic Corrosion at Al-Co Interface Uma Rames Krishna Lagudu, Ashwin M. Chockalingam, Laertis Eckonomikos et al.

Effect of MoO₃ buffer layer on the electronic structure of Al–BP interface

Baoxing Liu^{1,2}, Haipeng Xie^{1,*}, Shitan Wang¹, Yuan Zhao¹, Yuquan Liu¹, Dongmei Niu¹ and Yongli Gao³

E-mail: xiehaipeng@csu.edu.cn

Received 30 March 2022, revised 31 May 2022 Accepted for publication 20 June 2022 Published 30 June 2022



Abstract

The interfacial modification effect of the molybdenum trioxide (MoO₃) buffer layer inserted between Al and black phosphorus (BP) was investigated with photoemission spectroscopy. The results show that MoO₃ buffer layer can effectively prevent the destruction of the outermost BP lattice by Al thermal deposition and change the interface electronic structure between Al and BP. At the MoO₃/BP interface, there is an interface dipole pointing from MoO₃ to BP. During the metal deposition process, an interfacial chemical reaction between Al and MoO₃ was found. These observations would provide insight for fabricating high-performance BP-based devices.

1

Keywords: black phosphorus, aluminum, MoO₃, photoemission spectroscopy

(Some figures may appear in colour only in the online journal)

1. Introduction

Black phosphorus (BP) is a layered material with high carrier mobility and adjustable band gap, which has attracted wide attention in recent year [1–6]. BP is the most stable phase of phosphorus, and is allotrope with blue phosphorus and green phosphorus [7]. Unlike other two-dimensional (2D) materials, BP has a direct band gap, and its band gap shows a high dependence on its thickness [8–11]. In the electrical, optical, energy storage and other fields, BP-based devices are steadily emerging [12–19]. However, as an emerging 2D material, the practical application of BP still faces some challenges. Metals are widely used as electrodes in BP-based devices, and they may destroy the integrity of the BP lattice during the deposition process. According to our previous research, the outermost BP lattice can be destroyed in the early stage of deposition and unbond P atoms will appear in the Au/BP

and Co/BP interfaces [20, 21]. When Al is deposited on BP, a chemical reaction occurs and an Al–P compounds is formed, which changes the interface barrier height that is not conducive to carrier transport [22]. In order to reduce the damage of BP caused by metal deposition, a buffer layer is needed to be inserted at the metal/BP interface.

Molybdenum trioxide (MoO₃) is a very promising semiconductor metal oxide widely used for manufacturing fieldeffect transistors (FETs) [23], light-emitting diodes [24], solar cells [25–27], etc. Xiang *et al* demonstrated effective surface transfer electron and hole doping on BP FET devices through *in situ* surface functionalization with MoO₃ overlayers [23]. Even in the case of highly doped MoO₃ with a thickness of more than 10 nm, the hole mobility of the BP transistor remains almost unchanged, indicating that although the hole concentration of BP is greatly increased after doping with MoO₃, the scattering among the carriers can be ignored.

We used ultraviolet photoemission spectroscopy (UPS) and x-ray photoemission spectroscopy (XPS) to study the effect of a MoO_3 buffer layer on the electronic structure of the interface

¹ Institute of Super-Microstructure and Ultrafast Process in Advance Materials, School of Physics and Electronics, Central South University, Changsha, Hunan 410012, People's Republic of China

² College of Physics and Optoelectronic Engineering, Shenzhen University, Shenzhen 518060, People's Republic of China

³ Department of Physics and Astronomy, University of Rochester, Rochester, NY 14627, United States of America

^{*} Author to whom any correspondence should be addressed.

between Al and BP. The results show that MoO₃ buffer layer can effectively prevent the damage of BP crystal lattice caused by the metal deposition process and the interface electronic structure between Al and BP has been changed. There is an interface dipole at the MoO₃/BP interface. An interfacial chemical reaction between Al and MoO₃ was found in the process of metals deposition. The results can provide insight in designing BP-based electronic devices.

2. Experimental method

An ultra-high vacuum interconnection system was used to grow and test the samples in situ. In the preparation chamber, the BP crystal are mechanically peeled off with special tape inside a preparation chamber, and the pressure of the chamber is better than 2×10^{-8} mbar. In the experiment, MoO₃ and Al thin films were grown by thermal evaporation while the chamber pressure was better than 2×10^{-9} mbar. The deposition rates of MoO₃ and Al were 0.5 nm min⁻¹ and 0.05 nm min⁻¹ respectively. All deposition thicknesses were monitored by quartz crystal microbalance. The prepared BP is transferred in vacuum into the analysis chamber through the radial sample chamber, and its surface composition and crystal structure is detected by XPS (SPECS XR-MF) and low energy electron diffraction (LEED, SPECS ErLEED). The analysis chamber is equipped with a SPECS PHPIBOS 150 hemispherical energy analyzer, an ultraviolet light source (He I = 21.22 eV, Specs Microwave UV Light Source) and a monochromatic x-ray light source (Al K α = 1486.7 eV, Specs Microfocus x-ray source) [28–31]. All measurements were taken at room temperature.

3. Results and discussion

The layered crystal structure of BP is shown in figure 1(a), the atomic layers are superimposed by weak Van der Waals interaction like graphite, and the layer distance is about 5 Å [32]. Figure 1(b) is the LEED pattern of BP and the x and ycorrespond to armchair and zigzag direction respectively. The spot (0, 1) disappear in the LEED pattern due to the electron energy is 134 eV, and it appear when the electron energy drops to 90 eV [33]. Meanwhile, it is find that the ratio x/y is close to the BP lattice constant ratio a/b = 0.757, indicating that a clean BP surface was successfully obtained by mechanical exfoliation in the preparation chamber with an ultrahigh vacuum. The layered crystal structure of MoO₃ is shown in figure 1(c), where the Mo atoms are represented by gray spheres and O atoms by red spheres. The dotted line in the figure indicates the shape of MoO₃ single unit cell. Figure 1(d) shows the evolution of the P 2p peak of BP in the MoO₃/BP interface with the thickness of MoO₃. In order to have a more intuitive and clear vision for the position of P 2p core level, all the spectra will be normalized to the same height. The binding energy of the intrinsic BP P 2p peak is 130.32 eV. After deposition of 3 nm MoO₃, the P 2p peak disappears completely. During the whole deposition process, the position of the P 2p peak remained unchanged, and the peak width did not widen with

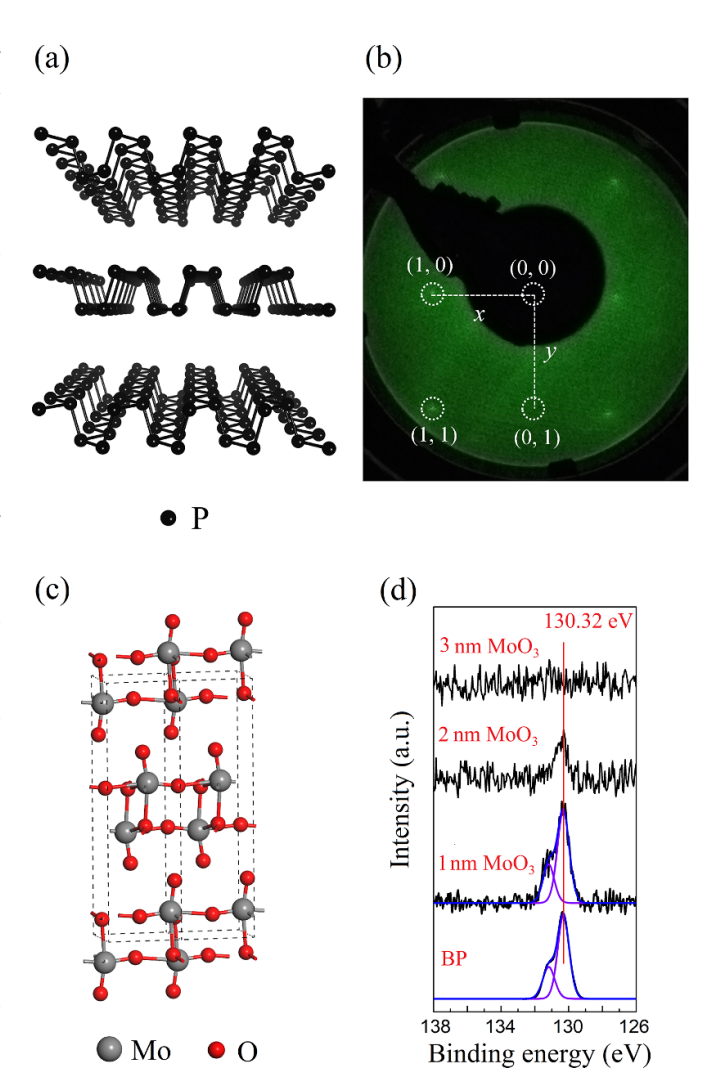


Figure 1. (a) Layered crystal structure of BP (lattice constant: a = 3.313 Å, b = 4.374 Å, c = 10.473 Å). (b) LEED diffraction pattern of BP. (c) Layered crystal structure of MoO₃. (d) The P 2p peak of BP evolves with the thickness of the MoO₃ film.

the increase of the thickness of MoO₃. No new peak was detected at higher and lower binding energy, indicating that BP was not oxidized or fragmented into unbound P atoms. Combining the XPS data of the Al/BP and the MoO₃/BP interface, it can be inferred that the MoO₃ deposition process is physical adsorption, not causing damage to the outermost BP lattice, in sharp contrast to the case of metal deposition [20, 21].

Figure 2 shows the UPS spectrum evolution with the thickness of the Al in the Al/MoO₃/BP interface. The work function (WF) of intrinsic BP is 4.24 eV. After deposition of 3 nm MoO₃, the WF changes to 6.33 eV. As an n-type semiconductor material with high WF, MoO₃ has a very significant modification effect on the BP interface. When the deposited thickness of Al is 1 Å, the WF is 5.21 eV. With the increase of the thickness of Al, the WF decreases gradually. After depositing 15 Å of Al, it reaches a minimum value of 3.54 eV, and the shift is 2.79 eV. As the thickness of Al further increases, the WF starts to increase and reaches 3.71 eV after depositing 30 Å Al, then the WF remains basically unchanged. Figure 2(b)

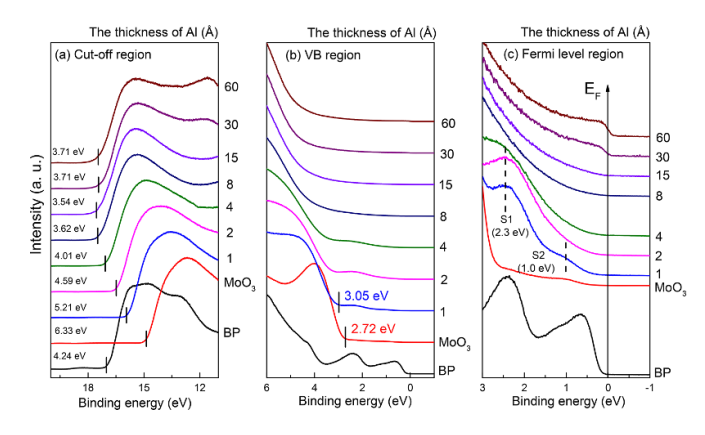


Figure 2. In the Al/MoO₃/BP interface, the UPS spectrum evolves with the Al thickness, (a) cut-off region, (b) valence band (VB) edge region, (c) the near Fermi level region of the valence band spectra as a function of Al thickness.

shows the VB edge region. It can be seen that the intrinsic BP has a valence band maximum (VBM) of 0.1 eV. After depositing 3 nm MoO₃, the VBM of MoO₃ film is measured to be 2.72 eV, which is consistent with the previous results [34]. Since the band gap ($E_{\rm gap}$) of MoO₃ is 3.10 eV [35], the conduction band minimum (CBM) of MoO₃ can be calculated as 0.38 eV using the formula $E_{\rm CBM} = E_{\rm gap} - E_{\rm VBM}$. As shown in figure 2(c), it is find that there are two interface states centered at about 2.30 and 1.00 eV respectively at low Al coverage (1–8 Å), and the metallic Fermi level cutoff begins to appear when the deposited thickness of Al reaches 30 Å.

In order to further understand the process of depositing Al on the MoO₃/BP thin film, we fitted the Al 2p, O 1s and Mo 3d spectra at different thicknesses in detail. The solid lines represent Gauss-Lorentz fitting results and the dashed lines represent original experimental data. Figure 3(a) shows the fitted Al 2p spectra. Based on the previous research results, we fit it with two peaks, the gray peak with higher binding energy corresponds to Al_xO. The orange peak with lower binding energy corresponds to metallic Al. When the thickness of Al is 1–8 Å, the binding energy of Al_xO peak increases gradually, indicating that the oxidation of Al was strengthened consequently. The metallic Al peak appears at a deposition thickness of 15 Å, and the Al_xO peak stabilizes at 75.59 eV. At 15–60 Å. The content of metallic Al peak increases gradually. Figure 3(b) shows the fitted O 1s spectra, where the red peak with lower binding energy corresponds to the oxygen component in MoO₃, and the blue peak with higher binding energy corresponds to the oxygen component in Al_xO. The binding energy of the oxygen component in MoO₃ is about 530.67 eV, and its position keeps unchanged but the content decreases gradually as the increase of the thickness of Al. It is worth noting that a new peak appear at high binding energy in the O 1s spectrum, which can be attributed to the oxygen component in Al_xO. Its position increases gradually and stays at 532.52 eV at 15-60 Å with the increase of the thickness of Al. Combining XPS and UPS data, it can be reasonably inferred that Al reacts with MoO₃ at the interface, which lead to the formation of interface states at low Al coverage (1-8 Å).

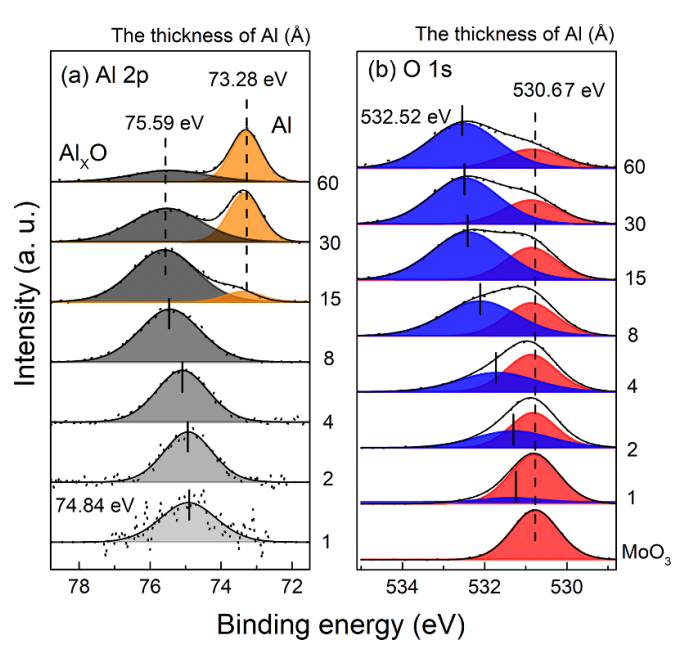


Figure 3. In the Al/MoO₃/BP interface, (a) Al 2p peak evolution with the thickness of the Al film. The gray peak corresponds to Al_xO and the orange peak corresponds to metallic Al. (b) O 1s peak evolution with the thickness of the Al film. The blue peak corresponds to the oxygen component in Al_xO, and the red peak corresponds to the oxygen component in MoO₃.

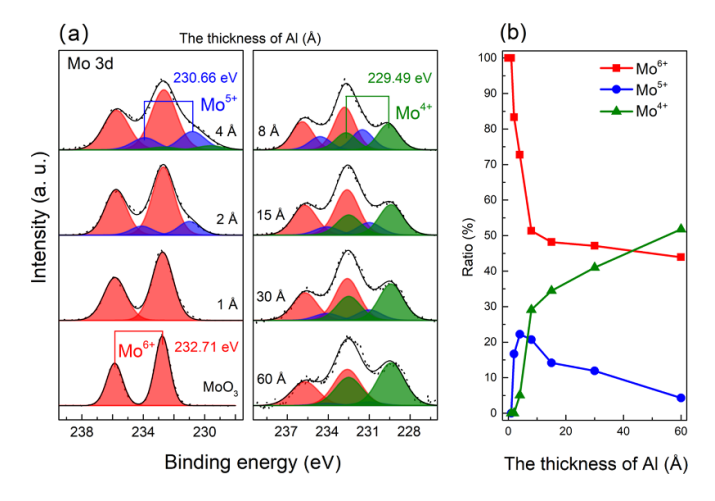


Figure 4. (a) In the Al/MoO₃/BP interface, the Mo 3d peak evolution with the thickness of the Al film, the red peak corresponds to $\mathrm{Mo^{6+}}$, the blue peak corresponds to $\mathrm{Mo^{5+}}$, and the green peak corresponds to $\mathrm{Mo^{4+}}$. (b) The ratios of Mo in $\mathrm{Mo^{6+}}$, $\mathrm{Mo^{5+}}$ and $\mathrm{Mo^{4+}}$ oxidation state vary with the thickness of Al.

Figure 4(a) shows the fitted Mo 3d spectra with different colors correspond to different Mo valence states. The red peak (232.71 eV) with higher binding energy corresponds to Mo⁶⁺, the blue peak (230.66 eV) corresponds to Mo⁵⁺, and the green peak (229.49 eV) with lower binding energy corresponds to Mo⁴⁺. The Mo 3d spectra is composed of Mo 3d_{3/2} and Mo 3d_{5/2} peaks, the energy interval is 3.08 eV and the area ratio is 2:3 [23, 34]. Only the Mo 3d_{5/2} peak is discussed as it is the most revealing. After depositing 3 nm MoO₃ on BP, the Mo 3d_{5/2} peak is located at 232.71 eV, and the valence state of Mo

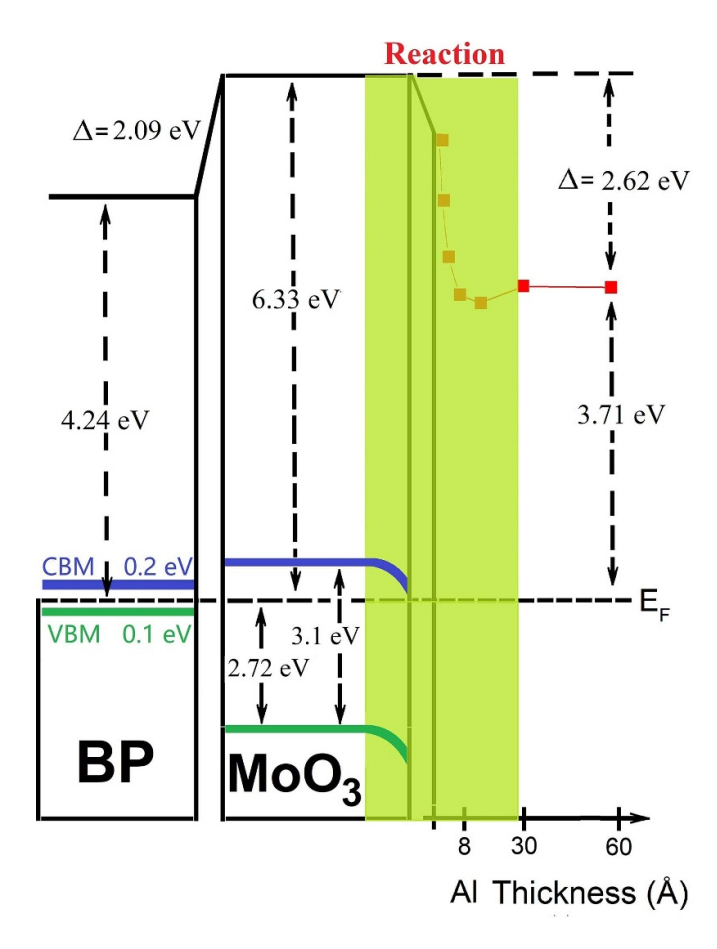


Figure 5. Al/MoO₃/BP interface energy level diagram.

is only Mo⁶⁺. When the deposition thickness of Al reaches 2 Å, Mo⁵⁺ oxidation state appears. When the thickness of Al reaches 4 Å, the Mo⁴⁺ oxidation state appears, with the thickness of Al increases, the proportion of Mo⁴⁺ increases rapidly. Figure 4(b) shows the proportion of Mo in Mo⁶⁺, Mo⁵⁺ and Mo⁴⁺ oxidation state varies with the thickness of Al. It can be seen that the proportion of Mo⁶⁺ decreased from 100% to 50% in the range of $1 \sim 8$ Å, indicating that a large amount of oxygen vacancies are generated in MoO₃. In the end, the proportion of Mo⁶⁺ decreased to 45%. The proportion Mo5+ increases first and then decreases as the thickness of Al increases, reaching a maximum at 4 Å, which is 23%. The proportion of Mo⁴⁺ monotonously increased during the whole deposition process. Due to the strong chemical activity of Al ions, a large amount of Mo⁶⁺ is directly reduced to Mo⁴⁺. At 60 Å, the proportion of Mo⁴⁺ increases to 52%. It indicated that the chemical reaction occurred between Al and MoO₃, in good agreement with the above discussions.

Figure 5 shows the energy level diagram of the Al/MoO₃/BP interface, where the WF data is obtained from figure 2(a). For intrinsic BP, its WF is 4.24 eV, VBM is 0.1 eV, and CBM is 0.2 eV. From the previous analysis, the MoO₃ deposition process is physical adsorption as no chemical reaction is observed. The WF of MoO₃ is 6.33 eV, the VBM is 2.72 eV, the CBM is 0.38 eV due to the band gap is 3.1 eV. There is an interface dipole of 2.09 eV at the

MoO₃/BP interface, and the direction of the interface dipole is from MoO₃ to BP. With the deposition of Al, a chemical reaction occurs at the Al/MoO₃ interface and there is an interface dipole of 2.62 eV at the interface, pointing from MoO₃ to the Al. The existence of interfacial dipoles with an electric field at the Al/MoO₃ interfaces would hinder to some extent hole extraction to the top electrode and reduce the short-circuit current [36]. After depositing 60 Å Al, the WF is 3.71 eV. In our previous work, it was found that the WF was 4.03 eV after the deposition of 60 Å Al [22]. Both of them are lower than that of pure Al, which can be attributed to the interface chemical reaction and a metallic mixture at these interface that has also been found in metal/pentacene interface [37]. Thus, the MoO₃ buffer layer can change the interface electronic structure between Al and BP.

4. Conclusions

In summary, the effect of the MoO₃ buffer layer on the electronic structure of the interface between metals and BP was investigated with XPS and UPS. We find that MoO₃ buffer layer can effectively prevent the damage of BP crystal lattice during metal deposition and the interface electronic structure between Al and BP has been changed. There is an interface dipole at the interface from MoO₃ to BP. A chemical reaction occurs at the Al/MoO₃ interface. The studies can provide assistance in designing BP-based electronic devices.

Data availability statement

All data that support the findings of this study are included within the article (and any supplementary files).

Acknowledgments

We thank the financial support by the National Natural Science Foundation of China (Grant No. 51802355) and the National Key Research and Development Program of China (Grant No. 2017YFA0206602). H X acknowledges the support by the Natural Science Foundation of Hunan Province (Grant No. 2018JJ3625). Y G acknowledges the support by the National Science Foundation (Grant No. DMR 1903962).

ORCID iDs

Haipeng Xie https://orcid.org/0000-0002-1220-4778

Dongmei Niu https://orcid.org/0000-0001-6993-4117

References

- [1] Li L, Yu Y, Ye G J, Ge Q, Ou X, Wu H, Feng D, Chen X H and Zhang Y 2014 Black phosphorus field-effect transistors Nat. Nanotechnol. 9 372–7
- [2] Xia F N, Wang H and Jia Y C 2014 Rediscovering black phosphorus as an anisotropic layered material for optoelectronics and electronics *Nat. Commun.* 5 4458

- [3] Ren X L, Lian P C, Xie D L, Yang Y, Mei Y, Huang X R, Wang Z R and Yin X T 2017 Properties, preparation and application of black phosphorus/phosphorene for energy storage: a review J. Mater. Sci. 52 10364–86
- [4] Zhao Y, Chen Y, Zhang Y H and Liu S F 2017 Recent advance in black phosphorus: properties and applications *Mater*. *Chem. Phys.* 189 215–29
- [5] Chen P F, Li N, Chen X Z, Ong W J and Zhao X J 2017 The rising star of 2D black phosphorus beyond graphene: synthesis, properties and electronic applications 2D Mater. 5 014002
- [6] Guo Z, Ding W D, Liu X W, Sun Z J and Wei L 2019 Two-dimensional black phosphorus: a new star in energy applications and the barrier to stability *Appl. Mater. Today* 14 51–58
- [7] Han W H, Kim S, Lee I H and Chang K J 2017 Prediction of green phosphorus with tunable direct band gap and high mobility J. Phys. Chem. Lett. 8 4627–32
- [8] Du Y L, Ouyang C Y, Shi S Q and Lei M S 2010 Ab initio studies on atomic and electronic structures of black phosphorus J. Appl. Phys. 107 093718
- [9] Prytz O and Flage-Larsen E 2010 The influence of exact exchange corrections in van der Waals layered narrow bandgap black phosphorus J. Phys.: Condens. Matter 22 015502
- [10] Narita S, Akahama Y, Tsukiyama Y, Muro K, Mori S, Endo S, Taniguchi M, Seki M, Suga S and Mikuni A 1983 Electrical and optical properties of black phosphorus single crystals *Physica B*+C 117 422-4
- [11] Maruyama Y, Suzuki S, Kobayashi K and Tanuma S 1981 Synthesis and some properties of black phosphorus single crystals *Physica B*+C **105** 99–102
- [12] Engel M, Steiner M and Avouris P 2014 Black phosphorus photodetector for multispectral, high-resolution imaging Nano Lett. 14 6414–7
- [13] Buscema M, Groenendijk D J, Steele G A, van der Zant H S and Castellanos-Gomez A 2014 Photovoltaic effect in few-layer black phosphorus PN junctions defined by local electrostatic gating *Nat. Commun.* 5 4651
- [14] Liu H, Neal A T, Zhu Z, Luo Z, Xu X, Tomanek D and Ye P D 2014 Phosphorene: an unexplored 2D semiconductor with a high hole mobility ACS Nano 8 4033–41
- [15] Qiao J, Kong X, Hu Z X, Yang F and Ji W 2014 High-mobility transport anisotropy and linear dichroism in few-layer black phosphorus *Nat. Commun.* 5 4475
- [16] Du Y, Liu H, Deng Y and Ye P D 2014 Device perspective for black phosphorus field-effect transistors: contact resistance, ambipolar behavior, and scaling ACS Nano 8 10035–42
- [17] Li L, Engel M, Farmer D B, Han S J and Wong H S 2016 High-performance p-type black phosphorus transistor with scandium contact ACS Nano 10 4672-7
- [18] Miao J, Zhang S, Cai L, Scherr M and Wang C 2015 Ultrashort channel length black phosphorus field-effect transistors ACS Nano 9 9236–43
- [19] Dai J and Zeng X C 2014 Bilayer phosphorene: effect of stacking order on bandgap and its potential applications in thin-film solar cells J. Phys. Chem. Lett. 5 1289–93
- [20] Liu B X, Xie H P, Niu D M, Huang H, Wang C, Wang S T, Zhao Y, Liu Y Q and Gao Y L 2018 Interface electronic structure between Au and black phosphorus J. Phys. Chem. C 122 18405–11

- [21] Liu B X, Xie H P, Liu Y Q, Wang C, Wang S T, Zhao Y, Liu J X, Niu D M, Huang H and Gao Y L 2020 Electronic structure and spin polarization of Co/black phosphorus interface J. Magn. Magn. Mater. 499 166297
- [22] Liu B X, Xie H P, Niu D M, Wang S T, Zhao Y, Liu Y Q and Gao Y L 2020 Interface electronic structure between aluminum and black phosphorus *Results Phys.* 18 103222
- [23] Xiang D et al 2015 Surface transfer doping induced effective modulation on ambipolar characteristics of few-layer black phosphorus Nat. Commun. 6 6485
- [24] Chu X B, Guan M, Zhang Y, Li Y Y, Liu X F and Zeng Y P 2013 ITO-free and air stable organic light-emitting diodes using MoO₃: pTCDAmodified Al as semitransparent anode RSC Adv. 3 9509–13
- [25] Sun G J, Shahid M, Fei Z P, Xu S D, Eisner F D, Anthopolous T D, McLachlan M A and Heeney M 2019 Highly-efficient semi-transparent organic solar cells utilising non-fullerene acceptors with optimised multilayer MoO₃/Ag/MoO₃ electrodes *Mater. Chem. Front.* 3 450–5
- [26] Latif H et al 2020 Effect of annealing temperature of MoO₃ layer in MoO₃/Au/MoO₃ (MAM) coated PbS QDs sensitized ZnO nanorods/FTO glass solar cell Sol. Energy 198 529–34
- [27] Wang F, Hu F, Zhang X and Xu H 2016 In-situ photoelectron spectroscopy investigation of interface coupling between metals and MoO₃ thin films Surf. Rev. Lett. 24 1750042
- [28] Xie H P, Huang H, Cao N T, Zhou C H, Niu D M and Gao Y L 2015 Effects of annealing on structure and composition of LSMO thin films *Physica* B 477 14–19
- [29] Xie H P, Liu X L, Lyu L, Niu D M, Wang Q, Huang J S and Gao Y L 2015 Effects of precursor ratios and annealing on electronic structure and surface composition of CH₃NH₃PbI₃ perovskite films *J. Phys. Chem.* C 120 215–20
- [30] Liu B X, Xie H P, Niu D M, Wang S T, Zhao Y, Liu Y Q, Lyu L and Gao Y L 2020 Effect of interfacial interaction on spin polarization at organic-cobalt interface *Org. Electron.* 78 105567
- [31] Xie H P, Niu D M, Lyu L, Zhang H, Zhang Y H, Liu P, Wang P, Wu D and Gao Y L 2016 Evolution of the electronic structure of C60/La_{0.67}Sr_{0.33}MnO₃ interface Appl. Phys. Lett. 108 011603
- [32] Lee T H, Kim S Y and Jang H W 2016 Black phosphorus: critical review and potential for water splitting photocatalyst *Nanomaterials* **6** 194
- [33] Wang C, Niu D M, Liu B X, Wang S T, Wei X H, Liu Y Q, Xie H P and Gao Y L 2017 Charge transfer at the PTCDA/black phosphorus interface J. Phys. Chem. C 121 18084–94
- [34] Zhu M L, Lu L, Niu D M, Hong Z, Wang S T and Gao Y L 2016 Effect of a MoO₃ buffer layer between C8-BTBT and Co(100) single-crystal film *RSC Adv.* 6 112403–8
- [35] Chen C W, Lu Y J, Wu C C, Wu E H, Chu C W and Yang Y 2005 Effective connecting architecture for tandem organic light-emitting devices Appl. Phys. Lett. 87 241121
- [36] Wu J, Guo X-Y and Xie Z-Y 2012 Effects of the molybdenum oxide/metal anode interfaces on inverted polymer solar cells *Chin. Phys. Lett.* 29 098801
- [37] Watkins N J, Yan L and Gao Y 2002 Electronic structure symmetry of interfaces between pentacene and metals Appl. Phys. Lett. 80 4384–6